Preparation and photoluminescence properties of Eu^{3+}, Y^{3+} co-doped Si nanowires

R. C. YANG[1], Z. D. FAN[1], X. P. GENG[1,*], G. L. WANG[2], F. WANG[3]
[1]*Department of Mathematics and Physics, Chengde Petroleum College, Chengde, 067000, China*
[2]*Student Affairs Department, Chengde Petroleum College, Chengde, 067000, China*
[3]*Department of Mechanical Engineering, Chengde Petroleum College, Chengde, 067000, China*

Using silicon nanowires as the groundmass of fluorescent nanomaterials, a series of Si nanowires co-doped with Y^{3+} and Eu^{3+} were prepared by high temperature method. The prepared fluorescent nanomaterials were characterized and analyzed by X-ray diffraction (XRD), scanning electron microscopy (SEM) and photoluminescence (PL). The results show that when the optimal excitation wavelength is 293 nm, the Y^{3+} , Eu^{3+} co-doped silicon nanowires have strong red emission, which is mainly characterized by a peak at 619 nm ($^5D_0 \rightarrow {}^7F_2$). At the same time, four emission bands of 576 nm ($^5D_0 \rightarrow {}^7F_0$), 596 nm ($^5D_0 \rightarrow$7F1), 658 nm ($^5D_0 \rightarrow {}^7F_3$) and 708 nm ($^5D_0 \rightarrow {}^7F_4$) were observed. When the molar ratio of Y^{3+}:Eu^{3+} is 2.5%, the emission intensity of Eu^{3+} red light is 110% higher than the case of no Y^{3+} doped. Analysis shows that Eu^{3+} occupies two positions of Y^{3+}:C_2 and S_6. The lack of reversal symmetry is conducive to the electric dipole transition, so the transition $^5D_0 \rightarrow {}^7F_2$ is enhanced. Furthermore, the full width at half maximum of red emission peak at 619 nm has been reduced from 10.2 nm to 7.2 nm, therefore the sensitivity and resolution of fluorescence detection is improved.

(Received May 29, 2018; accepted February 10, 2022)

Keywords: Photoluminescence, Eu^{3+},Y^{3+} co-doped, Si nanowires

1. Introduction

Eu^{3+} red emission has many advantages, such as stable physical properties, better monochromaticity and high quantum efficiency, therefore has been widely used in lighting, medicine, military, nuclear physics and radiation fields [1-4]. As a result, different kinds of Eu doped luminescent materials and preparation methods have been extensively studied nowadays. Lin [5] prepared Eu doped amorphous silicon oxycarbide (SiCO) films by magnetron sputtering followed by annealing. The results shows that the enhanced red/blue emission is due to the formation of high-density nanosized $EuSiO_3$ clusters, which enable energy transfer from nanosized $EuSiO_3$ clusters to Eu^{3+} and/or Eu^{2+} ions. Wang [6] synthesized Sr_3SiO_5:Eu^{3+} phosphors. It was found that the doping of BaF_2 improved the luminescence intensity of Sr_3SiO_5:Eu^{3+} and its temperature quenching performance. Game [7] successfully prepared phosphor $LiBaPO_4$:Eu^{3+} by the Pechini (citrate gel) method. In the wavelength range of 575-640 nm, there are two peaks at 595nm and 615nm, corresponding to the characteristic transitions $^5D_0 \rightarrow {}^7F_1$ and $^5D_0 \rightarrow {}^7F_2$ of Eu^{3+}, respectively, with the maximum intensity of 615 nm. Kumar [8] obtained a bright novel sensitized red emission from the functionalized multi walled carbon nanotubes embedded polymer nanocomposites Bi^{3+}+Eu^{3+}: PVA under UV excitation. Ramakrishna [9] investigated a series of Eu^{3+} doped Y_2SiO_5 red nanophosphors by eco-friendly combustion mode using Calotropis gigantea latex as a fuel. Under 397 nm excitation, the sample exhibits a strong red emission band with a peak at 612 nm, color coordinates of (0.5866, 0.4026) and an average correlation color temperature of 2018.5 K. These studies have important value for the development of photoluminescent materials, but the research on luminescent materials based on silicon nanowires is still unclear.

In this paper, silicon nanowires were used as the groundmass to obtain the luminescent materials by the way of mixed doping of elements, and their photoluminescence properties were studied, which contributed to the further use of luminescent materials. Silicon nanowires are used as the groundmass because silicon nanomaterials have many excellent properties. In particular, they can be biodegraded into low-toxic or non-toxic products and then cleared by the kidneys, which is greatly conducive to their application in bioscience. For example, there is great potential value for research on the occurrence, diagnosis, treatment of diseases in medicine and life sciences.

In addition, the large surface-to-volume ratio of silicon nanomaterials provides a great opportunity for drug delivery or biomolecular modification, and opens a new way for the design of high-performance silicon-based

multifunctional nano agents and nanoprobes. As the diameter of silicon nanowires becomes smaller and smaller, fluorescent nanomaterials based on silicon nanowires will have greater application value in the fields of ion recognition, fluorescent labeling, fluorescent imaging and medical diagnosis. Compared with bulk silicon, silicon nanowires, as the groundmass of fluorescent nanomaterials, have higher luminous efficiency.

This paper further prepared Eu^{3+},Y^{3+} co-doped SiNWs (denoted as SiNWs:Eu^{3+},Y^{3+}), considering the excellent luminescent properties when using silicon nanowires as the groundmass, and based on our extensive research on Eu^{3+} doped silicon nanowires(denoted as SiNWs:Eu^{3+}). A series of red emission tests were carried out, and the mechanism of Y^{3+} ions to enhance the luminescence intensity of Si was analyzed. The results show that the introduction of Y^{3+} ions has great impact on the enhancement of the luminescence intensity of SiNWs:Eu^{3+}.

2. Experiment

The SiNWs:Eu^{3+},Y^{3+} were prepared by the following steps.

Conventional chemical cleaning processes were used to treat n-(100) monocrystalline silicon with resistivity of 1.1-1.5 Ω•cm. 5-15 nm metal (Au-Al) catalyst was deposited on silicon substrate by vacuum evaporation coating machine. The high density silicon nanowires are grown from n-(100) monocrystalline silicon based on the solid-liquid-solid mechanism. Specifically, the samples are placed in a high temperature furnace, using Au-Al film as metal catalyst, and grown at 1100 ^{o}C for 30 min under the protection of 1.5 L/min nitrogen. The formed nanowires have a diameter of 50-300 nm and a length of several micrometers. A series of Y_2O_3 doped Eu_2O_3 powders were mixed into the alcohol and then spun onto the substrate with SiNWs by the spinning-coating process. The samples were dried in a drying oven. SiNWs:Eu^{3+},Y^{3+} were prepared by placing the sample in a high temperature furnace at a temperature of 1000 °C, N_2 flow rate of 1000sccm, and doping time of 60 min.

The morphology, microstructure, luminescent properties and crystal orientation of the SiNWs:Eu^{3+},Y^{3+} were characterized and analyzed by scanning electron microscopy (SEM), Hitachi F-4600 fluorescence spectrophotometer and X-ray powder diffraction (XRD).

3. Results and discussion

3.1. SEM and XRD

The diameters of the prepared SiNWs:Eu^{3+},Y^{3+} are 80-300 nm and the lengths vary from several micrometers. The SEM result is shown in Fig. 1(a) (the inset is a TEM image).

It can be seen that a large amount of powder exists on the SiNWs surface. The sample was also tested by XRD, and the result is shown in Fig. 1(b). The XRD spectrum peaks of SiNWs:Eu^{3+},Y^{3+} weakened compared to that of Eu_2O_3 standard cards (PDF#34-0392). At the same time, the XRD characteristic peaks of SiNWs:Eu^{3+},Y^{3+} become weakened or disappeared (* mark position) compared to that of SiNWs:Eu^{3+}. It can also be observed that new diffraction peak appeared at 44.4° of 2θ. During the software analysis, it is found that one of the Y_2SiO_5 spectral peaks is in good agreement with the single peak of the result. Because there is only a single peak, the XRD spectrum is not fully clear, and it is not very conclusive evidence. In addition, the reason for the weakening or the disappearance of different peaks and also the presence of only one peak for Y_2SiO_5 is not understood yet.

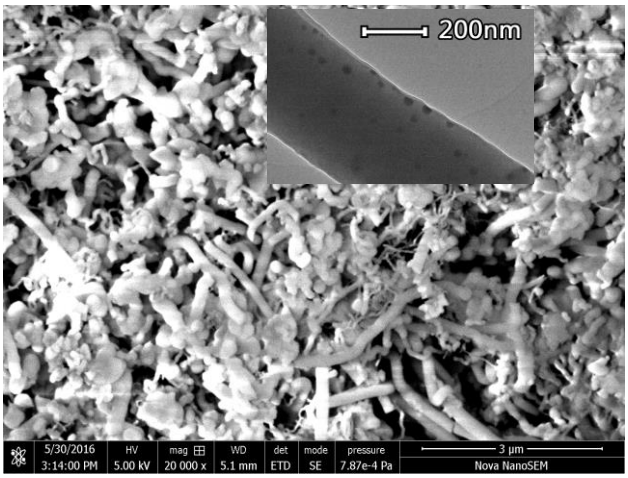

a)

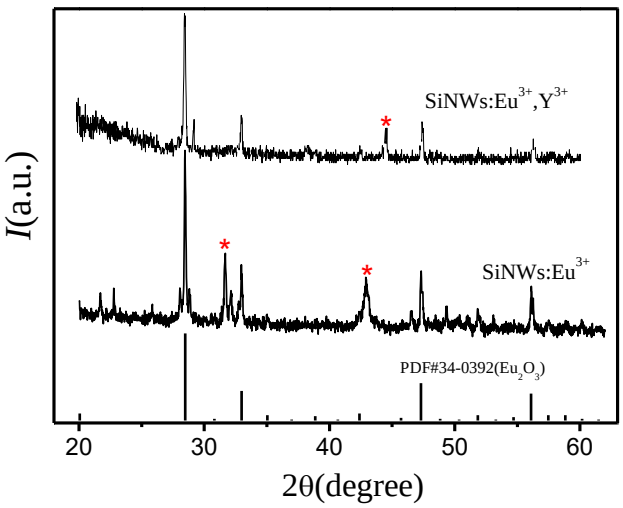

b)

Fig. 1. The SEM images (The inset is a TEM image) (a) and XRD spectrum (b) of SiNWs:Eu^{3+},Y^{3+}

3.2. PL properties

We have systematically studied the luminescence properties of SiNWs:Eu^{3+} [10]. From Fig. 2(a), it is observed that the peak of the excitation spectrum of the SiNWs:Eu^{3+} appears at 395 nm.

The experimental results of different substrates are shown in Fig. 2(b). Rare earth doped with bulk Si as the groundmass only produced extremely weak PL peak, while with Si nanowires as the groundmass, there is a strong PL peak. The analysis shows that Si nanowires have the characteristics of larger specific surface area and higher surface activity, which is conducive to the adsorption of rare earth ions on their surface and the formation of luminescence centers.

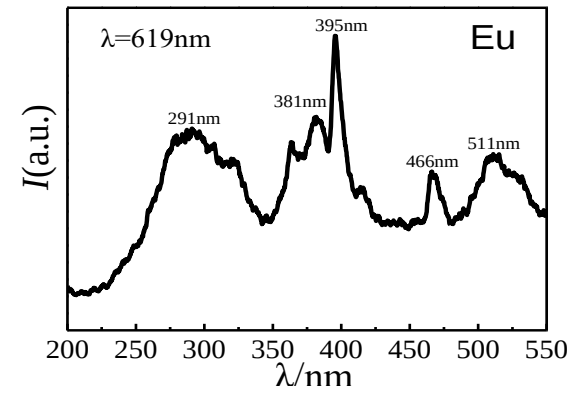

a)

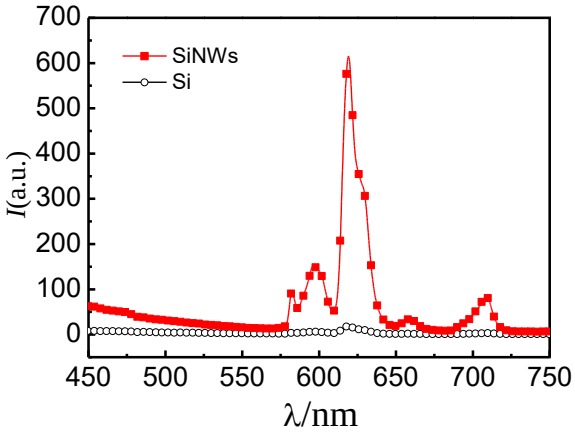

b)

Fig. 2. The excitation spectrum of Eu doped SiNWs (a) and emission spectrum of Eu doped bulk Si and SiNWs (b)

In order to further enhance the red light luminescence intensity, a series of SiNWs:Eu^{3+},Y^{3+} were prepared. The molar ratio of Y^{3+}:Eu^{3+} is 0-4.5% (for short Y^{3+} (0-4.5%). Their excitation spectra and emission spectra were test at room temperature, the results are shown in Fig. 3.

The excitation spectrum of the SiNWs:Eu^{3+},Y^{3+} has a strong and broad spectral peak in the range of 220-350 nm, which belongs to Eu^{3+}-O^{2-} charge transport band [11]. The peak of the spectrum is at 293 nm as Fig. 3(a) shows. The strong Eu^{3+}-O^{2-} charge transfer band appears because Y_2O_3 is a strong ionic crystal, and the perturbation of the crystal field significantly weakens the forbidden degree of 4f-4f electrons that are originally forbidden transitions, thus forming a strong excitation band [11]. The excitation peaks at 401 nm and 470 nm belong to the f-f transport of Eu^{3+}.

Fig. 3(b) shows the effect on the photoluminescence properties of the samples by ion doping with different molar ratios (0-4.5% indicated in the figure is the molar ratio of two ions, namely Y^{3+}: Eu^{3+}). The inset is a image of excitation light peak at different doping ratios of Y^{3+}.

With the increase of Y^{3+} doping ratio, the red emission intensity of the sample first increases and then decreases. When the ratio of Y^{3+}:Eu^{3+} reaches 2.5%, the luminous intensity reaches the maximum, which is about 110 % higher than the case of no Y^{3+} doped. As the Y^{3+} ratio further increases, the luminous intensity decreases due to the concentration quenching effect [12].

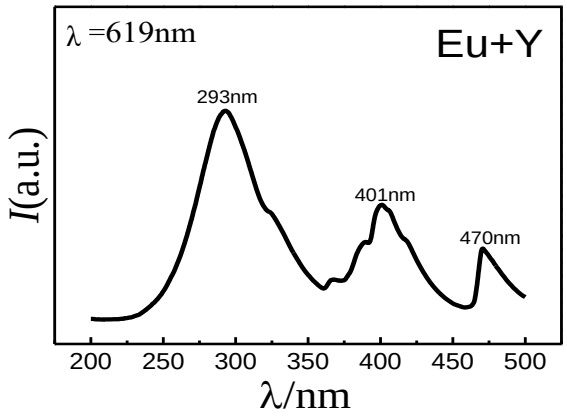

a)

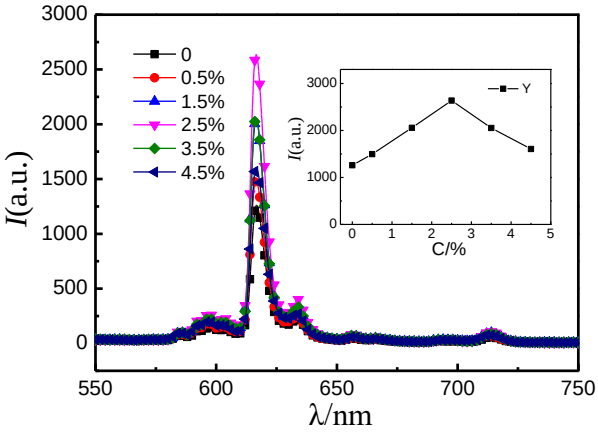

b)

Fig. 3. The excitation spectrum of Eu, Y doped SiNWs (a) and different ratio of Y doped SiNWs (The inset shows the light peaks at different Y^{3+}) (b) (color online)

3.3. Luminescence mechanism

It is well known that Y_2O_3 has a cubic crystal structure, the space group is Ia3(T_h^7)(NO.206) and the band gap is Eg=5.5eV. The valence band top is mainly composed of 2p electron state of O^{2-}, and the conduction band bottom is mainly composed of 4d electron state of Y^{3+} [13]. When Eu^{3+} is doped into the Y_2O_3, Eu^{3+} occupy two positions of Y^{3+}: C_2 and S_6 which was shown in Fig. 4 [2].

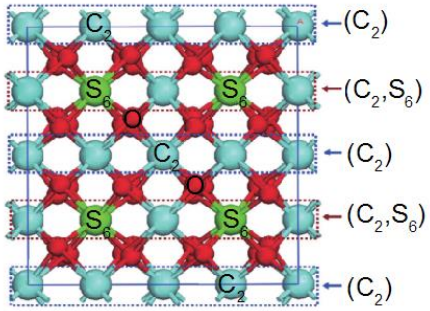

a)

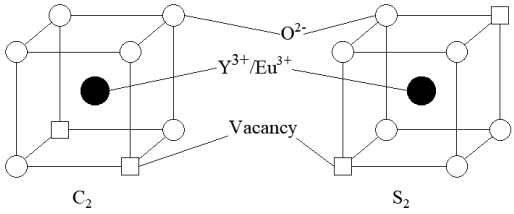

b)

Fig. 4. Schematic diagram of Y_2O_3 unit cell (a) (color online) and Eu^{3+} occupied Y^{3+} position (b)

Eu^{3+} absorbs ultraviolet light through the charge transport band and produce red light emission. Although S_6 has little contribution to red emission, it will compete with C_2 to absorb ultraviolet light. When Eu^{3+} occupies the C_2 position, because of the odd parity state, the atomic inversion center is missing. It is helpful to produce a strong electric dipole transition, leading to the $^5D_0$-$^7F_2$ (619 nm) energy level transition, which increases the red emission intensity of the sample [14]. The energy transfer diagram is shown in Fig. 5 [15], where V_0 is an oxygen vacancy. When exposed to ultraviolet light, Eu^{3+}-O^{2-} will absorb photon energy and produce charge transfer, i.e. Eu^{3+}-O^{2-}→Eu^{2+}-O^{1-}. Eu^{3+} is in an unstable state after absorbing an electron, then relaxes to $^5D_0$ level, and then transitions to ground state ^7F_j, resulting in different wavelengths of light emission.

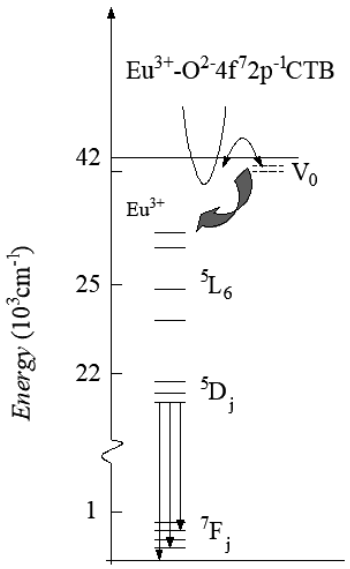

Fig. 5. Illustrated diagram of energy transmission

In this experiment, the strongest emission peak is at 619 nm, but the moral ratio of Eu^{3+} to Y^{3+} is very large. Therefore, the red light emission of Eu^{3+} has two parts. One is the light emission generated by Eu^{3+} occupying the C_2 and S_6 lattices of Y^{3+}, and the other is the light emission generated by the $^5D_0$→^7F_j transition of Eu^{3+} itself.

4. Conclusions

A series of SiNWs:Eu^{3+},Y^{3+} were prepared under the conditions of 1000 °C, 60 min doping time and 1000 sccm N_2 flow. Their excitation and emission spectra were tested at room temperature. The results show that the SiNWs:Eu^{3+},Y^{3+} have a strong red emission, and the main characteristic peak is at 619 nm ($^5D_0$→$^7F_2$). Four emission bands at 576 nm ($^5D_0$→$^7F_0$), 596 nm ($^5D_0$→$^7F_1$), 658 nm ($^5D_0$→$^7F_3$) and 708 nm ($^5D_0$→$^7F_4$) were observe. When the Y^{3+} doping ratio was 2.5%, the emission intensity of Eu^{3+} red light was 110% higher than the case of no Y^{3+} doped. The analysis showed that Eu^{3+} would occupy two positions of Y^{3+} :C_2 and S_6. The lack of reversal symmetry of C_2 is conducive to the electric dipole transition, so the transition $^5D_0$→$^7F_2$ is enhanced. In addition, the full width at half maximum of the red light emission peak at 619nm is reduced from 10.2 nm to 7.2 nm, which improves the sensitivity and resolution of fluorescence detection.

Acknowledgement

Supported by the Department of Science and Technology of Hebei Province of China (Grant No. 17211307).

References

[1] K. H. Jang, N. M. Khaidukov, V. P. Tuyen, S. II. Kim, Y. M. Yu, H. J. Seo, J. Alloy. Compd. **536**, 47 (2012).
[2] H. Cui, P. F. Zhu, H. Y. Zhu, H. D. Li, Q. L. Cui, Chin. Phys. B **23**, 568 (2014).
[3] D. D. Engelsen, P. Harris, T. Ireland, J. Silver, ECS J. Solid State SC. **4**, R1 (2015).
[4] R. S. Ukare, G. D. Zade, B. D. P. Raju, S. J. Dhoble, Optik **127**, 1871 (2016).
[5] Z. X. Lin, R. Huang, H. P. Wang, Y. Wang, Y. Zhang, Y. Q. Guo, J. Song, C. Song, H. L. Li, J. Alloy. Compd. **694**, 946 (2017).
[6] L. Wang, H. Ni, Q. Zhang, F. Xiao, Sci. Adv. Mater. **9**, 552 (2017).
[7] D. N. Game, C. B. Palan, N. B. Ingale, S. K. Omanwar, J. Mater. Sci. Mater. El. **28**, 8777 (2017).
[8] K. N. Kumar, R. Padma, L. Vijayalakshmi, J. S. M. Nithya, M. Kang, J. Lumin. **182**, 208 (2017).
[9] G. Ramakrishna, H. Nagabhushana, B. D. Prasad, Y. S. Vidya, S. C. Anantharaju, S. C. Prashantha, N. Choudhary, J. Lumin. **181**, 153 (2017).
[10] Z. D. Fan, Z. C. Zhou, C. Liu, L. Ma, Y. C. Peng, Acta Phys. Sin. **64**, 148103 (2015).
[11] A. P. Jadhav, A. Pawar, W. K. Chang, H. G. Cha, U. Pal, Y. S. Kang, J. Phys. Chem. C **13**, 16652 (2009).
[12] D. L. Dexter, J. H. Schulman, Journal of Chemical Physics **22**, 1063 (1954).
[13] J. W. Wang, Y. M. Chang, H. C. Chang, S. H. Lin, L. Huang, X. L. Kong, M. W. Kang, Chem. Phys. Lett. **405**, 314 (2005).
[14] Y. N. Xu, Z. Q. Gu, X. F. Zhong, W. Y. Ching, Phys. Rev. B **56**, 7277 (1997).
[15] M. Buijs, A. Meyerink, G. Blasse, J. Lumin. **37**, 9 (1987).

*Corresponding author: gxp5888@163.com